Variable Cosmological Constant model: the reconstruction equations and constraints from current observational data

Yin-Zhe Ma*
Kavli Institute for Theoretical Physics China, Institute of Theoretical Physics, Chinese Academy of Sciences (KITPC/ITP-CAS), P.O.Box 2735, Beijing 100080, People's Republic of China

In this paper we first give a brief review of the variable cosmological constant model and its scalar field description. We mainly discuss two types of variable cosmological constant models: a power law and H power law models. A method to obtain all of the equivalent scalar field potentials and the effective equation of state of the two models is presented. In addition, the dynamics of such scalar field potentials and effective equation of state are discussed in detail. The parameters of the two models are constrained by current 307 high-quality "Union" SN Ia data set, baryon acoustic oscillation (BAO) measurement from the Sloan Digital Sky Survey (SDSS), 9 observational H(z) data derived from the Gemini Deep Deep Survey (GDDS) and the shift parameter of the cosmic microwave background (CMB) given by the three-year Wilkinson Microwave Anisotropy Probe (WMAP) observations. We also calculate and draw the picture of the Hubble parameter, the deceleration parameter and the matter density of the two models. Then, we show that the indices m and n in the two models have specific meaning in determining properties of the models. Moreover, The reasons that indices m and n may also influence the behavior of effective equation of state and scalar field potentials are presented.

PACS numbers: 98.80.Cq, 98.65.Dx

I. INTRODUCTION

In 1998, the discovery that the accelerated expansion of the Universe is driven by the dark energy (DE) from the type Ia supernovae (SN Ia) observations [1] greatly astonished the world. The Wilkinson Microwave Anisotropy Probe [2], combined with more accurate SN Ia data [3] indicates that the Universe is almost spatially flat and the dark energy accounts for about 70% of the total content of the Universe. However, we know little about the nature of dark energy except for its negative pressure. Therefore, a large number of works have been done in recent years to explain this mystery.

The variable cosmological constant (hereafter VCC) [4] is one of the phenomenological ways to explain the dark energy problem, because it is a straightforward modification of the cosmological constant Λ which enable itself to be compatible with observations. Looking back to the history, we can see that a lot of theorists have done numerous works to search for the theoretical foundation of the VCC models and also investigate the properties of the VCC models [5]. In [6], a model of $\Lambda \propto a^{-2}$ was proposed, requiring that the cosmic density ρ would equal to the Einstein-de Sitter critical density ρ_c, which leads to a closed Universe, without singularity, horizon, entropy and monopoly problems [6]. After that, it was also suggested a model $\Lambda \propto a^{-2}$ (Λ should be independent of $\hbar$) with different initial conditions by [7], which firstly pointed out that time-dependent Λ leads to the creation of matter or radiation. Besides, a lot of work were done to propose straightforward models relating Λ to the Hubble parameter $H(z)$: $\Lambda \propto H^2$ [8, 9, 10, 11]. Furthermore, people also constructed a large number of phenomenal VCC models to describe the dynamics of the Universe and there is a list in Ref. [4] summarizing the proposed models [12]. There are also several papers concerning the observational constraints about the VCC models [13].

In addition to the VCC models, scalar fields such as "quintessence" [14], "phantom" [15] and "quintom" [16] have been introduced to effectively describe the dynamic dark energy, which are distinguished by the effective equation of state (hereafter EEoS): $w_{DE} > -1$, $w_{DE} < -1$ and w_{DE} across -1 respectively. These models are inspired by the fact that a decaying vacuum energy which has the very high energy density at early time should be sufficiently small at present to meet the current observation requirement, so they should evolve dynamically. In order to obtain the corresponding quintessence potentials, the reconstruction equations were derived and addressed the feasibility of the approach by Monte-Carlo simulation [17]; it was also constructed the general scalar-field dark energy model [18] and developed a method to construct them directly from EEoS function $w_\phi(z)$ [19, 20]. Moreover, some works have been done to reconstruct the scalar potential from the scalar-tensor theory and investigate the modified Newton theory [21].

As a major part of our work, we analyze the EEoS and reconstruct the potentials for two main types of VCC models—— the a power law and the H power law models—— from the point of view of dynamic scalar fields. This work is necessary for people who are interested in the coupled dark energy and dark matter [22], because such models may avoid a lot of realistic problems such as the coincidence problem. In addition, it is discussed

*Electronic address: mayinzhe@itp.ac.cn

how such phenomenological models can be explained as a classical scalar field decaying into a perfect fluid which might be interested by those who want to search for the gravitational theory other than the general relativity, because the Lagrangian in VCC should be different from the Einstein-Hibert action in general relativity. Thus, this part should be essential for people to see the possible forms of VCC models and its corresponding scalar fields which are expected from string theory or supergravity.

Another main part of this paper is to give an observational constraint on the VCC models and explain the properties of cosmological parameters. This part of work is the basic analysis to determine the right form of VCC models from the observational requirement.

This paper is organized as follows: in section 2, we search for the EEoS, the reconstruction equation and effective potentials for all the a power law models, generalizing previous work from Ref. [23]. Next, we use the current observational data, including 307 high-quality "Union" SN Ia data set, baryon acoustic oscillation from SDSS, 9 observational H(z) data and CMB shift parameter from WMAP three years result, to constrain the index in this model. In addition, we analyze the properties of the dark energy density, the dark matter density and the deceleration parameter in this model. In section 3, parallelling to section 2, we generalize the work from Ref. [23] and discuss the EEoS, the reconstruction equation and reconstructed potentials for all of the H power law models. In addition, we also give one example of this type of model to prove the effectiveness of our method. Then, we use data to constrain the cosmological parameters of this type of models and analyze the properties of the dark matter density, Hubble parameter and the deceleration parameter. The concluding remark will be presented in the last section.

II. a POWER LAW MODELS AND CORRESPONDING POTENTIALS

For a generalized VCC related to the scale factor a, we can write

$$\Lambda = Ba^{-m}, \tag{1}$$

where B is a constant with the dimension of mass square and we call it the dark energy amplitude. We assume the VCC is proportional to the scale factor power $-m$, and power index m plays a significant role in determining the dark energy behavior as discussed below. Then, the dark energy density and the Friedmann equation can be written as (Note that $a_0 = 1$, $\frac{d}{dt} = -H(1+z)\frac{d}{dz}$.)

$$\rho_\Lambda^{(a)}(z) = \Lambda M_{pl}^2 = B(1+z)^m M_{pl}^2. \tag{2}$$

$$3M_{pl}^2 H^2 = \rho_m^{(a)} + \rho_\Lambda^{(a)}. \tag{3}$$

For simplicity of calculations we assume spatial flatness ($k = 0$) which is motivated by theoretical considerations, such as inflation, and also confirmed by current observations such as WMAP three years result [2]. Our results can be easily generalized to the case with a spatial curvature. We denote $M_{pl} = (8\pi G)^{-\frac{1}{2}}$ as the reduced Planck mass and use superscript (a) here to denote a power law model, we will also use superscript (H) to denote H power law model in the next section. $\rho_m^{(a)}$is the dust matter density with the present value

$$\rho_{m0}^{(a)} = 3H_0^2 M_{pl}^2 \Omega_{m0}. \tag{4}$$

Thus, we get

$$B = 3H_0^2(1 - \Omega_{m0}). \tag{5}$$

In our practice, there is clearly only one degree of freedom in the a power law model, which is the power index m. As for the VCC models, it is rather natural to consider the interaction between the dark matter and dark energy [24]. Therefore, we should introduce an interacting term $Q(z)$ with

$$\dot{\rho}_m^{(a)} + 3H\rho_m^{(a)} = Q(z), \tag{6}$$

$$\dot{\rho}_\Lambda^{(a)} + 3H(\rho_\Lambda^{(a)} + p_\Lambda^{(a)}) = -Q(z), \tag{7}$$

and the total energy conservation equation

$$\dot{\rho}_{tot} + 3H(\rho_{tot} + p_{tot}) = 0, \tag{8}$$

still holds. Since VCC is the generalized from of cosmological constant, so it satisfies $p_\Lambda^{(a)} = -\rho_\Lambda^{(a)}$. The Eq. (7) leads to

$$Q(z) = -\dot{\rho}_\Lambda^{(a)} = A(1+z)^m H, \tag{9}$$

where

$$A = 3H_0^2(1 - \Omega_{m0})mM_{pl}^2, \tag{10}$$

which means that the interaction is explicitly determined only by the evolution of dark energy density.

A. Interacting dark energy and reconstructed potentials in the a power law models

The anterior Eqs. (6) and (7) are the standard interacting dark energy equations and the function $Q(z)$ represents the interaction between dark energy and dark matter. Since the interaction may not be directly observable, it is interesting to search for the phenomenologically equivalent potentials which encode some properties of the interaction.

One way to search for such a theory is to express the VCC models in a field theory language, so the most straightforward way might be the scalar field description. If one could find such a description of the VCC models, it is natural to extend the scalar field description to other

space-time and other gravitational theory like superstring theory. In addition, this description is very useful since it provides a path to quantize the scalar field, which can help people to understand the fundamental theory of the phenomenological VCC models. Furthermore, the procedure to obtain a scalar field description of a phenomenological model could be applied to other models.

From this point of view, we want to see what are the EEoS and dark energy potentials in the a power law models. Changing the form of Eq. (7), we have

$$\dot{\rho}_\Lambda^{(a)} + 3H(\rho_\Lambda^{(a)} + p_\Lambda^{(a)} + \frac{Q(z)}{3H}) = 0, \tag{11}$$

so we could see the interaction $Q(z)$ contribute to the effective pressure

$$\begin{aligned} p_{eff}^{(a)} &= p_\Lambda^{(a)} + \frac{Q(z)}{3H} \\ &= -\rho_\Lambda^{(a)} + \frac{Q(z)}{3H}, \end{aligned} \tag{12}$$

so the EEoS of dark energy is

$$\omega_{eff}^{(a)} = \frac{p_{eff}^{(a)}(z)}{\rho_\Lambda^{(a)}(z)} = \frac{m}{3} - 1, \tag{13}$$

so we obtain this result from the point of view of interacting dark energy [20, 25]. In Eq. (13), the power index m is a constant, so the EEoS in the a power law models are all constants. We will see in the following subsection that the best-fit of index m constrained by current combined observational data is -0.09, which means $\omega_{eff}^{(a)} < -1$, so VCC is phantom-like [15]. However, for 2σ confidence level we cannot rule out the possibility that $m > 0$ (quintessence-like), so we should consider both the phantom and quintessence scalar field potentials for the VCC model.

For a spatially homogeneous and isotropic scalar field, the effective energy density $\rho_\Lambda^{(a)}$ and pressure $p_{eff}^{(a)}$ can be written as

$$\mp \frac{1}{2}\dot{\phi}^2 + V_{eff}^{(a)}(\phi) = \rho_\Lambda^{(a)}, \tag{14}$$

$$\mp \frac{1}{2}\dot{\phi}^2 - V_{eff}^{(a)}(\phi) = p_{eff}^{(a)}, \tag{15}$$

respectively, where upper (lower) sign represents the phantom (quintessence) scalar field, and $V_{eff}^{(a)}(\phi)$ is the effective scalar field potential for the a power law models. At the same time, the effective energy density $\rho_\Lambda^{(a)}$ and pressure $p_{eff}^{(a)}$ are given by the interacting dark energy equations

$$\rho_\Lambda^{(a)} = A_1(1+z)^m, \tag{16}$$

$$\begin{aligned} p_\Lambda^{(a)} &= -\rho_\Lambda^{(a)} + \frac{Q(z)}{3H} \\ &= A_2(1+z)^m, \end{aligned} \tag{17}$$

where

$$A_1 = 3H_0^2 M_{pl}^2(1-\Omega_{m0}), \tag{18}$$

and

$$A_2 = A_1(-1 + \frac{m}{3}). \tag{19}$$

We define the dimensionless quantities

$$\tilde{\phi} \equiv \phi/M_{pl},\ \tilde{V}_{eff} = V_{eff}/3H_0^2M_{pl}^2. \tag{20}$$

Thus, the scalar field potential can be written as a function of redshift z

$$\begin{aligned} \tilde{V}_{eff}^{(a)}(z) &= \frac{1}{2}(\rho_\Lambda^{(a)} - p_{eff}^{(a)}) \\ &= A_3(1+z)^m. \end{aligned} \tag{21}$$

where

$$A_3 = (1-\Omega_{m0})(1-\frac{m}{6}). \tag{22}$$

Combining Eqs. (14) and (15), we have

$$\frac{d\tilde{\phi}}{dz} = \mp \frac{C_1}{(1+z)[C_2 + C_3(1+z)^{3-m}]^{\frac{1}{2}}}, \tag{23}$$

where

$$C_1 = (1-\Omega_{m0})^{\frac{1}{2}} \times [|m|\,(3-m)]^{\frac{1}{2}}, \tag{24}$$

$$C_2 = 3(1-\Omega_{m0}),\ C_3 = (3\Omega_{m0} - m). \tag{25}$$

The upper (lower) sign in Eq. (23) represent $\dot{\phi} > 0$ ($\dot{\phi} < 0$). In fact, the sigh is arbitrarily determined by assumption, as it can be changed by $\phi \to -\phi$. We choose the upper sign in the following discussion. If we shift ϕ_0 value, the potential in the following figure will be shifted horizontally, but the shift doesn't influence the whole shape of the potential. The field could be integrated analytically as

$$\tilde{\phi}(z) = C_4 \times \tanh^{-1}[\frac{C_2^{\frac{1}{2}}}{(C_2 + C_3(1+z)^{3-m})^{\frac{1}{2}}}], \tag{26}$$

where

$$C_4 = \frac{2}{\sqrt{3}}[\frac{|m|}{3-m}]^{\frac{1}{2}}. \tag{27}$$

We let the integral constant equals to zero since the initial value of field is meaningless. Solving this for $(1+z)$ and substituting the result into (21), we obtain the potential of the a power law model

$$\tilde{V}_{eff}^{(a)}(\tilde{\phi}) = A_3[\frac{C_2}{C_3} \times (\coth^2(\frac{\tilde{\phi}}{C_4}) - 1)]^{\frac{m}{3-m}}. \tag{28}$$

We use the best fits value for m in the next section to

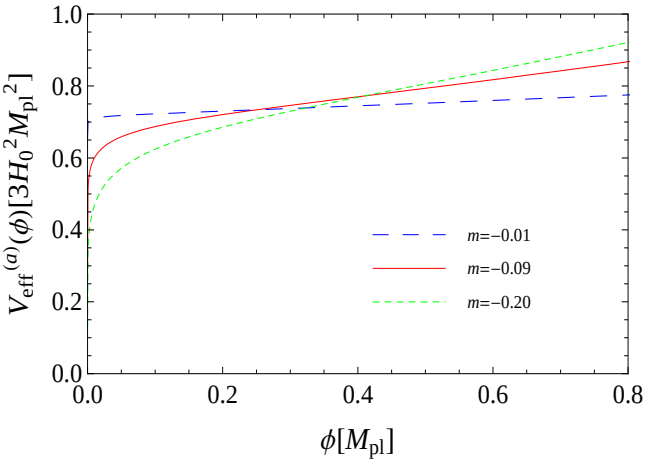

FIG. 1: Reconstructed potentials for a power law model. Here we set $\Omega_{m0} = 0.28$.

draw the pictures for the a power law models' equivalent potentials. There are three main characteristics for these potentials: First, they are all runaway type and the whole shape doesn't change if ϕ is shifted horizontally. Second, Eqs. (21) and (26) determine that ϕ increases and $V_{eff}^{(a)}(\phi)$ increases as the redshift z decreases from large value to -1, which means that the dark energy potentials increase as the Universe expands. From the figure, we could see that more negative the value of m is, the sharper the potentials will increase as the field evolves. One of the possible explanation for this phenomenon is that the more negative value of m means the dark matter "decays" into dark energy quicker, so the dark energy increase its potential value and energy density faster. Third, the hyperbolic *coth* function in the expression (28) makes the a power law potentials have the asymptotic value. This is very interesting because one could obtain such behavior in general in the supersymmetric QFT. This runaway form of potential is also the one expected in the unstable D-brane system in superstring theory [26].

B. Hubble parameter and results of the constraints on m

In this subsection, we want to constrain the parameter m from combined observational data, so we should obtain the Hubble parameter and the luminosity distance. We can change the variable t to redshift z in the Eq. (6) to figure out the analytical expression for the matter density

$$\rho_m^{(a)}(z;m) = 3H_0^2M_{pl}^2[D_1(1+z)^3 + D_2(1+z)^m], \quad (29)$$

where

$$D_1 = \frac{C_3}{3-m},\ D_2 = \frac{m}{3-m}(1-\Omega_{m0}). \quad (30)$$

We can easily note that the effect of VCC is just like a small perturbation to the evolution of the matter density. If the evolution behavior of the matter density doesn't deviate much from $(1+z)^3$ behavior (ΛCDM), the value of m should be very near zero, which indicate that even though the dark energy is not constant through the evolution of the Universe, it at least should evolve very slow. This property will be convinced through observational constraints on power index m in the following subsection. This equation is essential for our purpose to solve the Hubble parameter in the following subsection.

As there is only one free parameter in this kind of power law models, it is rather easy to obtain the best fit value from the current observational data. We do this fitting using the high quality type Ia supernovae, baryon acoustic oscillation from SDSS, observational $H(z)$ data and the the shift parameter of the cosmic microwave background (CMB) given by WMAP three years results. We discuss this problem in the framework of interacting dark energy and accelerating Universe (see relevant work [27]).

Integrating the Eq. (3), we have the following equation

$$H(z) = H_0[D_1(1+z)^3 + D_3(1+z)^m]^{\frac{1}{2}}, \quad (31)$$

where

$$D_3 = \frac{C_2}{3-m}. \quad (32)$$

Then we integrate the Eq. (31) and follow the guideline in Appendix (B) to obtain the χ^2 formula to do numerical fitting. Our result is much tighter than the previous fitting results [27] due to the more precise data we use. Under the combined data sets SN+BAO+OHD+CMB constraints, the 3σ values for the power index m are

$$m = -0.09^{+0.08+0.12+0.19}_{-0.11-0.20-0.29}. \quad (33)$$

From the above results, we are still not able to rule out the positive m value within 2σ confidence level, so we need more precise data to constrain the VCC models' power index in the future. However, no matter whether the m is negative or positive, it is very near zero, suggesting that even though the dark energy is not a constant, it should evolve very slow. The results for the best-fit and 1σ values are shown in Table 1. From our results, the Ω_{m0} is always around 0.28, which is consistent with the WMAP three years results [2].

C. Matter density and deceleration parameter of the a power law models

Having the matter density Eq. (29) and the confidence region of parameter m, we can plot the matter density and dark energy density as a function of redshift z as FIG. 3 and FIG. 4 shows. We put the curve representing the standard matter density equation in ΛCDM model for comparison.

Models		SN+BAO	SN+BAO+OHD	SN+BAO+OHD+CMB
a power	m	$-0.12^{+0.40}_{-0.42}$	$-0.19^{+0.29}_{-0.32}$	$-0.09^{+0.08}_{-0.11}$
law	Ω_{m0}	$0.28^{+0.03}_{-0.04}$	$0.28^{+0.04}_{-0.03}$	$0.29^{+0.03}_{-0.07}$
H power	n	$-0.26^{+0.67}_{-0.74}$	$-0.76^{+0.24}_{-0.74}$	$-0.15^{+0.14}_{-0.17}$
law	Ω_{m0}	0.28 ± 0.04	0.27 ± 0.03	0.29 ± 0.03

TABLE I: Results of the fitting for the two models.

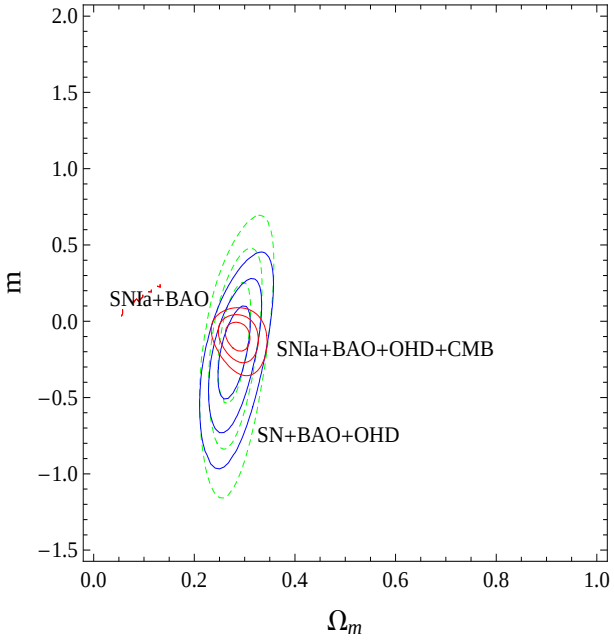

FIG. 2: Contour map for the parameter m versus Ω_{m0} in the a power law model. Green dashed lines represent SN+BAO, blue lines represent SN+BAO+OHD, and red lines represent SN+BAO+OHD+CMB.

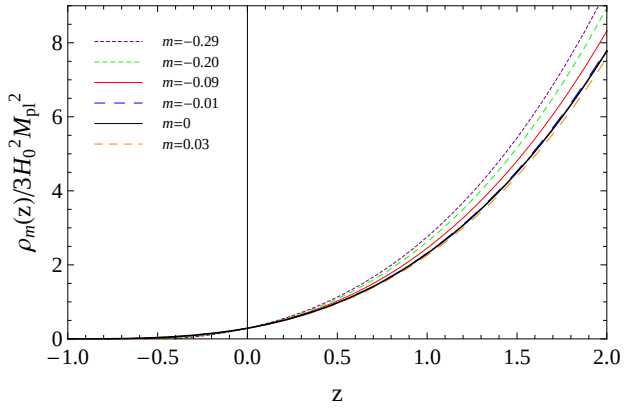

FIG. 3: Matter density for a power law models. Here we set $\Omega_{m0} = 0.28$.

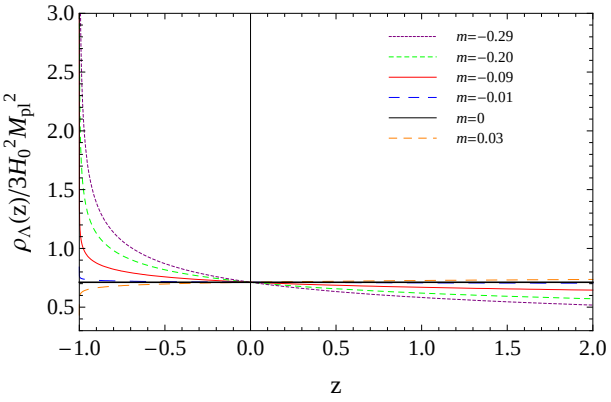

FIG. 4: Dark energy density for a power law models. Here we set $\Omega_{m0} = 0.28$.

From FIG. 3 and 4, if m is positive, the dark energy density changes and slower the matter density decreases as a function of redshift z. That means the dark energy "decays" into dark matter field and makes the matter dilute more slowly with the cosmic expansion, vice versa. As a result, the dark energy density will continuously decrease as the Universe evolves. On the contrary, if $m < 0$, the dark matter transforms into dark energy and the dark matter energy density decreases more sharply than the usual $(1+z)^3$ behavior (ΛCDM). Then the dark energy increases its energy density and realizes the "Big Rip" in the future due to this matter changes, so effectively it resembles the phantom dark energy (see Eq. (13)).

It is easy to see this property of index m through the "decay rate" ϵ in Ref. [29]. The "decay rate" ϵ is defined as the matter density's deviation from the standard evolution, i.e.,

$$\rho_m = \rho_{m0} a^{-3+\epsilon}, \tag{34}$$

where ρ_{m0} is the current matter density. In our case, ϵ is not a constant but a function of redshift z. In addition, it is straightforward to verify that m is the index to distinguish the sign of ϵ, as $m > 0$, $\epsilon(z) > 0$; vice versa. Thus, the relationship between index m and the "decay rate" ϵ represents whether the dark energy "decays" into dark matter or the inverse. Moreover, it is also easy to confirm that the value of $\epsilon(z)$ is generally compatible with the confidence region provided by [29].

Having obtained some meaning of the index m and its confidence region in the a power law models, we can directly find the evolution of the deceleration parameter

in this kind of model.

$$q^{(a)}(z) = -\frac{\ddot{a}a}{\dot{a}^2} = -\frac{1}{2}\frac{2-m-D_4(z)}{D_4(z)+1}, \tag{35}$$

where

$$D_4(z) = \frac{C_3}{C_2}(1+z)^{3-m}. \tag{36}$$

From FIG. 5, we can understand the following characteristics about the deceleration parameter in the a power law models: First, different a power law behaviors (including ΛCDM) have common deceleration parameters at present time $q(0) = \frac{3}{2}\Omega_{m0} - 1$. Second, they have different values of redshift z when the Universe was changing from deceleration to acceleration, so the transition redshift z_T for different models are determined by the following equation

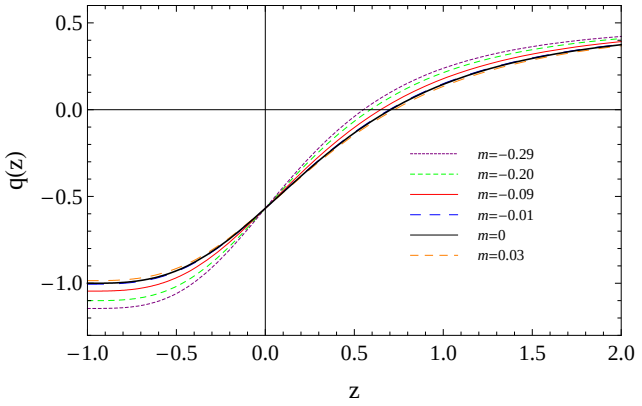

FIG. 5: Deceleration parameter for a power law models. Here we set $\Omega_{m0} = 0.28$.

$$z_T = [\frac{(2-m)C_2}{C_3}]^{\frac{1}{3-m}} - 1, \tag{37}$$

which can be determined by the results of the constraints. In addition, we could calculate the different z_T corresponding to m as the best fit, 1σ, 2σ confidence values and the ΛCDM: $z_T(m=-0.29) = 0.57$, $z_T(m=-0.20) = 0.61$, $z_T(m=-0.09) = 0.67$, $z_T(m=-0.01) = 0.72$, $z_T(m=0.03) = 0.75$. So the larger m is, the earlier the Universe changes from deceleration to acceleration. Thus, we obtain this transition redshift z_T from the general a power law form and the results should be applicable for all of the specific power law behaviors [29]. Third, the more negative value of m is, i.e., more sharply dark energy density changes, the faster Universe accelerates. This result is also compatible with the FIG. 3 in [29].

Furthermore, we can also use the constraints on the deceleration parameter and transition redshift to see whether our results are consistent with relevant constraints[30, 31, 32]. In Ref. [30], it shows that the best fits for the transition redshift is $z_T = 0.78^{+0.08}_{-0.27}$. Our results are rather consistent with this work because this best fits value for z_T will lead to the best fits region for m $[-0.43, 0.16]$, and our 3σ results for m is just within this region, suggesting that our constraints on m and Ω_{m0} are very tight. At the same time, our results are also very consistent with other relevant constraints on the "equivalent" redshift when $\rho_m(z_{eq}) = \rho_\Lambda(z_{eq})$ [31].

Therefore, in this subsection we conclude that the power index m of the a power law model is not only associated with the dark energy density, but also a meaningful index to determine whether the dark matter "decays" into dark energy or the inverse. Moreover, it determines the "decay rate" ϵ, i.e., the intensity by which dark matter changes into dark energy. Meanwhile, it affects the deceleration parameter of the Universe and the transition redshift z_T when the Universe was changing from deceleration to acceleration.

III. H POWER LAW MODEL AND ITS RECONSTRUCTED POTENTIALS

In this section, we will discuss another type of VCC models—— Λ is associated with Hubble parameter H—— which is an important type presented in Ref. [4].

In this type of model, the VCC can be written as

$$\Lambda = CH^n, \tag{38}$$

where C is a constant with the dimension of mass $2-n$, n is the only parameter in this kind of models which needs to be fitted by observational data. Then, the dark energy density and the Friedmann equation in this model can be given by

$$\rho_\Lambda^{(H)} = \Lambda M_{pl}^2 = CH^n M_{pl}^2, \tag{39}$$

$$3M_{pl}^2 H^2 = \rho_m^{(H)} + \rho_\Lambda^{(H)}. \tag{40}$$

The amplitude C is determined by the current value of matter density and the Hubble constant

$$C = 3H_0^{2-n}(1-\Omega_{m0}). \tag{41}$$

Then, we consider that the VCC indicates that there is an interaction between the dark matter and dark energy. Therefore, let's assume that dark energy and matter exchange pressure through the interaction term $W(z)$ with

$$\dot{\rho}_m^{(H)} + 3H\rho_m^{(H)} = W(z), \tag{42}$$

$$\dot{\rho}_\Lambda^{(H)} + 3H(\rho_\Lambda^{(H)} + p_\Lambda^{(H)}) = -W(z), \tag{43}$$

which maintains the total energy conservation equation $\dot{\rho}_{tot} + 3H(\rho_{tot} + p_{tot}) = 0$. Since the VCC is the generalization of the cosmological constant, so it should satisfy $\rho_\Lambda^{(H)} = -p_\Lambda^{(H)}$, then Eq. (43) leads to

$$\begin{aligned} W(z) &= -\dot{\rho}_\Lambda^{(H)} \\ &= G_1 H^n (1+z) H'(z), \end{aligned} \tag{44}$$

where

$$G_1 = 3nH_0^{2-n}(1-\Omega_{m0})M_{pl}^2. \tag{45}$$

A. Interacting dark energy and reconstructed potentials in the H power law model

In this subsection, we want to see the potential that dark energy mimics the VCC. Although the interaction between dark energy and dark matter might not be directly observable, the effective potential could encode some information about the interaction. Thus, we are looking forward to solving the EEoS and reconstruct the dark energy potentials of the H power law models from the standard interacting dark energy Eqs. (42) and (43).

Transforming Eq. (43), we have

$$\dot{\rho}_\Lambda^{(H)} + 3H(\rho_\Lambda^{(H)} + p_\Lambda^{(H)} + \frac{W(z)}{3H}) = 0, \tag{46}$$

from which the interaction changes the effective pressure of this model, i.e.

$$p_{eff}^{(H)} = p_\Lambda^{(H)} + \frac{W(z)}{3H}, \tag{47}$$

so the EEoS of dark energy is

$$\omega_{eff}^{(H)} = \frac{p_{eff}^{(H)}}{\rho_\Lambda^{(H)}} = -1 + \frac{n}{2}\frac{G_2(z)}{G_2(z)+G_3}, \tag{48}$$

where

$$G_2(z) = \Omega_{m0}(1+z)^{3(1-\frac{1}{2}n)}, G_3 = (1-\Omega_{m0}). \tag{49}$$

These EEoS are functions of redshift z, in contrast to the a power law models, where the EEoS is constant in the Eq. (13). It is quite interesting that the sign of index n also determines whether this dark energy likes the quintessence or phantom. Moreover, this type of EEoS is affected by the value of Ω_{m0}, while the EEoS in the a power law models are not. Since the constraint from the current observational data suggests that the best-fit for n is negative but cannot rule out the possibility of positive constant n (see discussion in next section), we construct the potentials for the two cases. The energy density and pressure density of the quintessence field for this model are

$$\mp\frac{1}{2}\dot{\phi}^2 + V_{eff}^{(H)}(\phi) = \rho_\Lambda^{(H)}, \tag{50}$$

$$\mp\frac{1}{2}\dot{\phi}^2 - V_{eff}^{(H)}(\phi) = p_{eff}^{(H)}. \tag{51}$$

where the upper (lower) sign represents the phantom (quintessence) dark energy, corresponding to $n < 0$ ($n > 0$). At the same time, we can obtain the expressions for dark energy density and pressure through definition (39) and the interacting dark energy Eq. (43).

$$\rho_\Lambda^{(H)} = A_1[G_2(z)+G_3]^{\frac{n}{2-n}}, \tag{52}$$

$$\begin{aligned} p_\Lambda^{(H)} &= -A_1[G_2(z)+G_3]^{\frac{2(n-1)}{2-n}} \\ &\times [(1-\frac{n}{2})G_2(z)+G_3]. \end{aligned} \tag{53}$$

Then, the effective scalar potential can be written as a function of redshift z

$$\begin{aligned} \tilde{V}_{eff}^{(H)}(z) &= G_3[G_2(z)+G_3]^{\frac{2(n-1)}{2-n}} \\ &\times [(1-\frac{n}{4})G_2(z)+G_3]. \end{aligned} \tag{54}$$

Using the Eqs. (50) and (51), we can obtain the differential form of scalar field

$$\frac{d\tilde{\phi}}{dz} = \mp\frac{G_4(1+z)^{\frac{1}{2}-\frac{3}{4}n}}{G_2(z)+G_3}, \tag{55}$$

where

$$G_4 = (\frac{3}{2}|n|)^{\frac{1}{2}}(\Omega_{m0}(1-\Omega_{m0}))^{\frac{1}{2}}. \tag{56}$$

In general, Eq (55) could be solved analytically so we obtain the following field equation

$$\tilde{\phi}(z) = \tilde{\phi}_0 \mp G_5 \arctan[G_6(1+z)^{\frac{3}{2}(1-\frac{1}{2}n)}], \tag{57}$$

where

$$G_5 = \frac{2}{2-n}(\frac{2}{3}|n|)^{\frac{1}{2}}, G_6 = (\frac{\Omega_{m0}}{1-\Omega_{m0}})^{\frac{1}{2}}, \tag{58}$$

and the upper(lower) sign applies if $\dot{\phi} > 0$ ($\dot{\phi} < 0$). In fact, the sigh is arbitrarily determined by assumption, as it can be changed by $\phi \to -\phi$. We substitute $(1+z)$ for ϕ into Eq. (54) to get the result of potential $\tilde{V}_{eff}^{(H)}(\tilde{\phi})$.

$$\tilde{V}_{eff}^{(H)}(\tilde{\phi}) = G_3^{\frac{2}{2-n}}[1+\tan^2(\frac{(\tilde{\phi}-\tilde{\phi}_0)}{G_5})]^{\frac{2(n-1)}{2-n}}. \tag{59}$$

We give the following three examples of phantom potentials for this kind of models (see FIG. 6). As is shown in FIG. 6, the effective phantom potentials also have some characteristics: For one thing, they are all runaway type potentials and even if we change the initial value $\tilde{\phi}_0$, the curves shift horizontally with the whole shape unchanged. For another thing, the meanings of the potentials are clear: as the Universe is expanding, the value of ϕ becomes large and the field slowly rolls upon the potential, which makes the EEoS very close to -1. At the same time, the dark matter field gradually "decays" into dark energy, so the dark energy density increases its energy density as the Universe expands.

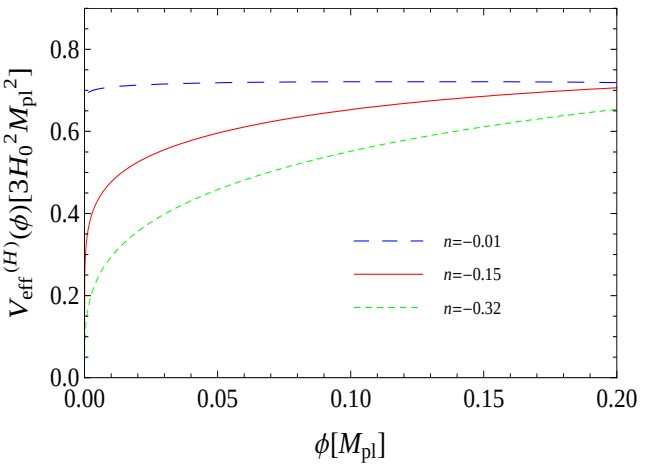

FIG. 6: Reconstructed potentials for H power law model. Here we set $\Omega_{m0} = 0.28$.

B. One specific examples of reconstructed potentials for the H power law models

In Ref. [4], there is a list of proposed H power law models proposed by different authors through various perspectives. In addition, Ref. [23] gives two examples of scalar potentials from the point of view of the scalar field description. In order to show the effectiveness of our reconstruction, we derive one analytic results of the scalar potentials using the methods in previous subsection.

$n = 2$ is an interesting [8] case of the VCC model and investigated by many authors [4, 23]. We substitute $n = 2$ into Eq. (54) to obtain

$$\tilde{V}_{eff}^{(H)}(z) = (1 - \Omega_{m0})(1 - \frac{1}{2}\Omega_{m0})(1 + z)^{3\Omega_{m0}}, \qquad (60)$$

and the field (55) could be integrated as

$$\tilde{\phi}(z) = \tilde{\phi}_0 - 3G_7 \ln(1 + z), \qquad (61)$$

where $\tilde{\phi}_0$ is the initial value of field $\tilde{\phi}$ and

$$G_7 = \Omega_{m0}(1 - \Omega_{m0}). \qquad (62)$$

Thus, we obtain the potential by substituting $(1 + z)$ for field $\tilde{\phi}$

$$\tilde{V}_{eff}^{(H)}(\tilde{\phi}) = (1 - \Omega_{m0})(1 - \frac{1}{2}\Omega_{m0})e^{-\alpha(\tilde{\phi}-\tilde{\phi}_0)}, \qquad (63)$$

where $\alpha = (\frac{3\Omega_{m0}}{1-\Omega_{m0}})^{\frac{1}{2}}$. This form is rather consistent with that in Ref. [23], which demonstrates the effectiveness of the reconstructing method in this paper. This potential is one of the simplest runaway types which represents the particle creation in the phenomenological VCC models so it could be interpreted as some kind of "coupled quintessence" [22]. Meanwhile, it is also easy to see that all the VCC potentials are associated with the exponential function, which leads to its runaway behavior, indicating that they might be easily obtained in supergravity and unstable D-brane systems [26].

C. Hubble parameter and results of the constraints on n

From Eqs. (40), (42) and (44), we can obtain the differential equation for the Hubble parameter

$$H^{'}(z) - \frac{1}{2(1+z)}(3H - K_1 H^{n-1}) = 0, \qquad (64)$$

where

$$K_1 = 3H_0^{2-n}(1 - \Omega_{m0}). \qquad (65)$$

The Eq. (64) can be solved analytically

$$H(z) = H_0[G_2(z) + G_3]^{\frac{1}{2-n}}. \qquad (66)$$

Then, we follow the procedure in Appendix (A) and (B) to do the numerical fitting and finally we can find 1σ results as Table 1 shows. Under the combined SN+BAO+OHD+CMB constraints, the best fit, $1\sigma, 2\sigma$ and 3σ values for parameter n is

$$n = -0.15^{+0.14+0.23+0.25}_{-0.17-0.26-0.43}. \qquad (67)$$

From the result (67), no matter whether n is negative

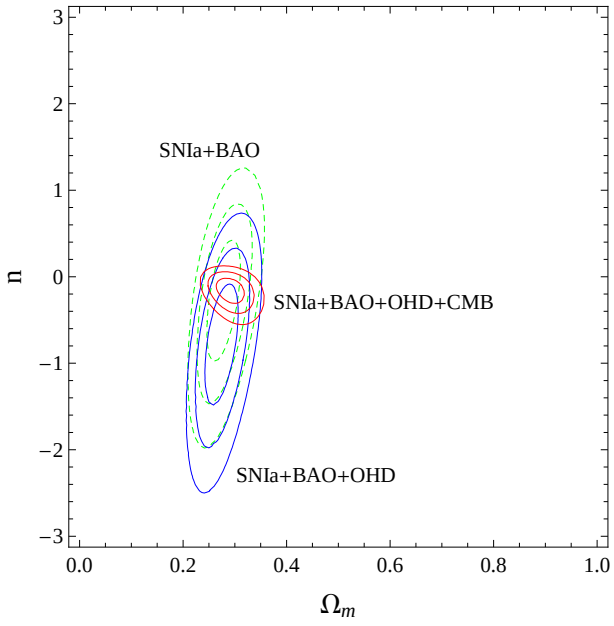

FIG. 7: Contour map for the parameter n versus Ω_{m0} in the H power law model. Green lines represent SN+BAO, blue lines represent SN+BAO+OHD, and red lines represent SN+BAO+OHD+CMB.

or positive, it always very near 0, indicating the slow evolution of dark energy. We could plot the EEoS (48) as a function of redshift z and compare them with other models [28] and observational results [33]. This EEoS has three major properties: For one thing, the confidence region of this type of models is mildly consistent with the

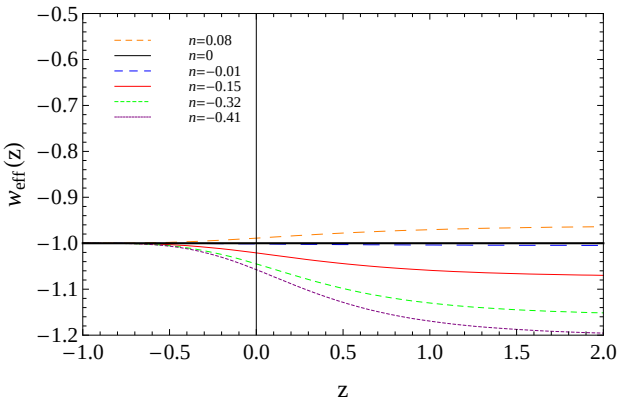

FIG. 8: The redshift dependence of the EEoS for H power law models. Here we set $\Omega_{m0} = 0.28$.

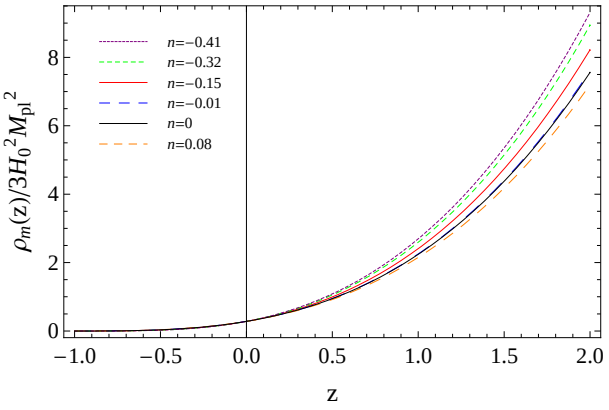

FIG. 9: Matter density for H power law models. Here we set $\Omega_{m0} = 0.28$.

results which were obtained by using CMB and Clusters data [33], indicating that it is a competitive model waiting for the examination by future observations. For another thing, within 1σ confidence region, the EEoS is slightly less than -1, which implies that it resembles the phantom field. In contrast, within 2σ region it is possible that the EEoS is greater than -1, so we cannot rule out the possibility that the dark energy is quintessence like. Thus, this type of models could really represent a large kind of dark energy models phenomenologically. Further more, if z become larger, all of the EEoS in these models have their own asymptotically constant value, which is rather similar to that of the "quiessence model" [34]. The constant EEoS means that the proportion of kinetic energy to potential energy is constant. Thus, the whole dark energy density increases or decreases, suggesting that the VCC models corresponds to a dissipative system of dark energy [5, 6, 22]. When redshift z approaches -1, all of the EEoS $w_{eff}(z)$ approach -1, indicating the Universe will enter the de-Sitter phase in the future.

D. Matter density, Hubble parameter and deceleration parameter of the H power law models

From the Hubble parameter Eq. (64), we can obtain the matter density

$$\rho_m^{(H)}(z;n) = 3H_0^2 M_{pl}^2 G_2(z)[G_2(z) + G_3]^{\frac{n}{2-n}}. \qquad (68)$$

Then, we plot the dark matter density and Hubble parameter of the H power law model. In order to compare with ΛCDM model, we also plot $n = 0$ curve in one graph. Thus, FIG. 9 helps us to analyze the properties of the matter density in this model: For one thing, we can see that for the positive n, the dark energy density decreases and the matter density dilutes more slowly as the Universe evolves, vice versa. On the contrary, $n < 0$ represents the dark matter changes into dark energy because the dark energy density increases as time evolves and the corresponding curve (for example, the curve in the graph $n < 0$) decreases more sharply than the standard $(1+z)^3$ behavior (ΛCDM). As a result, the parameter n is not only a power index of the H power law models, but also an important signature to distinguish whether dark energy "decays" into dark matter or the inverse process, just as the index m in the a power law case. Further more, comparing FIG. 9 and FIG. 3, we can discover that the two graphs are very similar to each other, which means that the two types of VCC models—— the a power law and the H power law models—— really share some common features if the parameters are all constrained by observational data. This could be understood as follows: both the scale factor $a(t)$ and the Hubble parameter $H(z)$ describe the evolution of the Universe; if the Universe is expanding canonically, $a(t)$ will increase while the $H(z)$ will decrease, so the difference between the two types might only lie in the sign of the power index.

However, if we plot the Hubble parameter by selecting some ideal value of n, we could see that they indicate the different fates of the Universe. We see from Fig. (10)

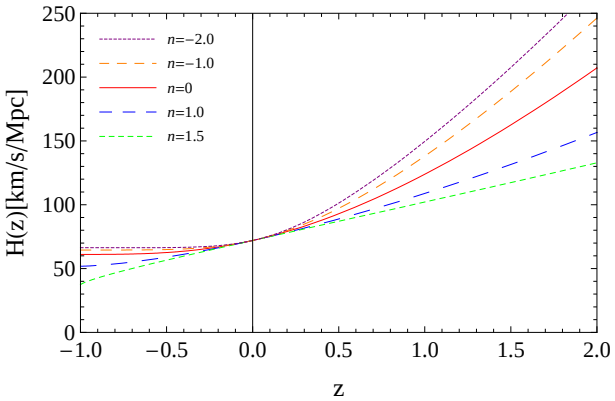

FIG. 10: Hubble parameter for H power law models. Here we set $\Omega_{m0} = 0.28$ and $H(0) = 72$km/s/Mpc.

that for any selected value of n, the Hubble parameter cannot deverge, so the H power law model does not in-

dicate the "Big Rip" phase in the future. This property could be understood from Fig. (8), because whatever the current value of w_{eff} is, they will all tend to be -1, so the Universe will enter a de-Sitter phase in the future. This property is rather different from a power law model since w_{eff} is a constant in that model, so the dark energy will be always a phantom if $m < 0$, which surely results in a phantom Universe with the "Big Rip" phase in the future (see Fig. (4)).

Having obtained the matter density, we can derive the deceleration parameter in this model

$$q^{(H)}(z) = -\frac{1}{2}\frac{2 - K_2(z)}{1 + K_2(z)}, \tag{69}$$

where

$$K_2(z) = \frac{\Omega_{m0}}{1 - \Omega_{m0}}(1 + z)^{3(1-\frac{1}{2}n)}, \tag{70}$$

Then, we can plot this deceleration parameter and also compare the curves with that of ΛCDM. From FIG. (11),

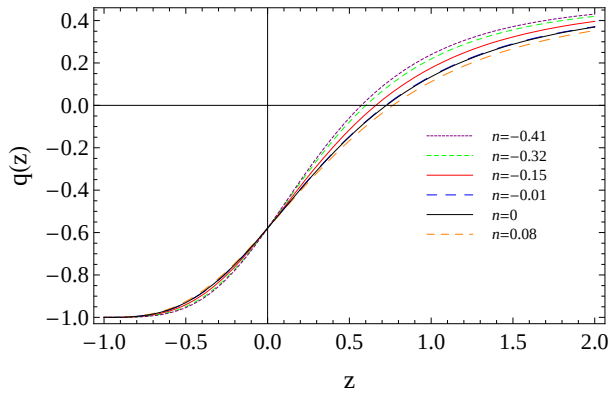

FIG. 11: Deceleration parameter for H power law models. Here we set $\Omega_{m0} = 0.28$.

we could analyze the properties of the deceleration parameter in this H power law model. For one thing, just as the a power law case, all of the H power law models share the same deceleration parameter at present time, which is $q(0) = \frac{3}{2}\Omega_{m0} - 1$, but they also share the same deceleration parameter values in the future ($a \to \infty$) as $q(z = -1) = -1$, which is different from that of the a power law model. For another thing, transition redshift z_T varies differently according to the different curves, which indicates that different values of n affect the expansion of the Universe distinctively. The transition redshift z_T for different models are determined by the following equation

$$z_T = [\frac{2(1 - \Omega_{m0})}{\Omega_{m0}}]^{\frac{2}{3(2-n)}} - 1. \tag{71}$$

We could calculate its value with respect to different index n numerically (see Table 2). It is also easy to see that the value of z_T within 1σ confidence region is generally compatible with the result in Ref. [29]. In addition, from Fig. (11), the transition redshift is in the range $[0.57, 0.77]$, which is just in the best fits region of transition redshift in Ref. [30] and [31], indicating that our numerical constraints on the parameters n has been already very tight compared with relevant work [30, 31, 32]. Moreover, different values of n correspond to different curves with distinctive shapes. For one thing, within 1σ region, n is definitely negative (such as $n = -0.15$), this makes the dark energy density increases and dark matter "decays" into dark energy as time evolves. The more negative the index n is, the more quickly the dark energy density $\rho_\Lambda^{(H)}$ increases and the faster the Universe accelerates. For another thing, within 2σ confidence region, there is a certain probability that the index n is positive, which indicates that the density of dark energy is decreasing, so the acceleration is relatively small compared to the negative value of n. To conclude this subsection, we derive the evolution of the matter density, Hubble parameter and the deceleration parameter in the H power law models. We note that the index n is just like the index m in the a power law models, which not only reflects whether the dark energy "decays" into dark matter, but also affects the acceleration of the Universe—— the deceleration parameter $q(z)$ and transition redshift z_T.

IV. CONCLUDING REMARKS

In this paper, we develop a method to reconstruct potentials in the VCC models directly from the definition of the energy density and pressure of the scalar field. We also give one example of the reconstruction for the H power law models. First, these potentials have some relationship with the exponential function, which is expected in supersymmetry theory and unstable D-brane system in superstring theory [26]. Second, as the Universe is expanding, the value of ϕ becomes large and the field slowly rolls upon the potential. At the same time, the dark matter field gradually "decays" into dark energy, so the matter density dilutes more sharply than the standard $(1 + z)^3$ behavior. It is worth noticing that the reconstruction equations presented here are not limited to searching for the scalar field description of such phenomenological VCC models. Generally, it could give people the possibility to find the scalar field versions of other phenomenological models and even quantum gravity models such as holographic models [35] and vacuum fluctuation model [36].

We also investigate constraints on the VCC models—– the a power law and the H power law models—— from current combined cosmological observations, using high quality supernovae, baryon acoustic oscillation from SDSS, observational H(z) data derived from Gemini Deep Deep Survey (GDDS) and the CMB shift parameter from WMAP three years result. We consider a spatially flat FRW Universe with matter component and VCC component. For the VCC models, such as the a power law and the H power law models, the power indices m and n play

n	$-0.41(2\sigma)$	$-0.32(1\sigma)$	-0.15(the best fit)	$-0.01(1\sigma)$	$0(\Lambda\text{CDM})$	$0.08(2\sigma)$
z_T	0.57	0.60	0.66	0.72	0.73	0.77

TABLE II: transition redshift z_T in H power law model.

a very significant role in determining the evolutionary behavior of the space-time as well as the ultimate fate of the Universe. According to the combined constraints, the best fit, 1σ, 2σ and 3σ values for the indices m and n are $m = -0.09^{+0.08+0.12+0.19}_{-0.11-0.20-0.29}$, $n = -0.15^{+0.14+0.23+0.25}_{-0.17-0.26-0.43}$ respectively. These results cannot fix the value of m and$n$, but at least indicate even though the dark energy may change with time, it will evolve very slow since the value of m and$n$ are always very near zero. The indices of VCC models suggest the interaction between dark energy and dark matter: First, $m > 0$ and $n > 0$ represent that the dark energy "decays" into dark matter, while $m < 0$ and $n < 0$ represent the inverse process. The more negative the indices m and n are, the faster such transitions happen. Second, the indices m and n affect the deceleration parameter and the transition redshift z_T. The more negative the indices m and n are, the more portion dark energy takes in the whole Universe budget in the future due to the matter "decays"; thus, faster the Universe will be accelerating. Also, the more negative the indices m and n are, the less portion they took into the whole Universe budget in the past and the smaller value of transition redshift z_T is. Therefore, the indices m and n are the important signatures to judge whether the Universe accelerates more drastically than the ΛCDM model. Third, the indices m and n are also the essential indicators to understand the properties of VCC. For one thing, the best fit values for m and n suggest that the EEoS of dark energy are real numbers or functions of redshift z at the region $[-1.5, -1]$, indicating that the dynamic scalar fields of VCC are phantom-like. For another thing, there are still some probabilities for the a power law and the H power law models that the dynamic scalar field of VCC is quintessence-like, so the VCC models are the phenomenal models representing a variety of other dynamic dark energy models. Moreover, the EEoS of the a power law models are constant, while those of the H power law models are functions of redshift z but have the asymptotic values when redshift z becomes large, so at the early stage, the VCC models have some properties of the quiessence model. The different fate indicated by the two models are, if redshift z tends to be -1, the EEoS in H power tends to be -1, so the Universe enter a de-Sitter phase in the future. However, the EEoS of a power law model is always a negative constant, indicating the Universe will enter the "Big Rip" phase in the future.

The cosmological constant problem is still one of the serious problem that puzzles the physical world and we are still far away to go to its nature. Thus, we expect that a more sophisticated combined analysis of various observations will be capable of determining the indices value of VCC models and revealing more properties of the VCC dark energy models.

Acknowledgments

The author would like to thank Hui Li, Rong-Gen Cai, Shi Qi, Tan Lu, Yan Gong and Yong-Shi Wu for helpful discussion. He also thanks Guo-Xing Ju, Hao Yin, Lei Zhang, Nan Zhao and Tie-Yan Si for helpful direction of computer program and Hao Wei, Hong-Sheng Zhang, Hui Li, Li-Ming Cao, Xing Wu for revision and Yan Gong for suggesting high quality supernovae data sets. This work was supported partially by grants from NSFC, China (No. 10325525, No. 90403029 and No. 10525060) and a grant from the Chinese Academy of Sciences.

APPENDIX A: SOME RESULTS OF INTEGRALS

We define a dimensionless function

$$E(z) \equiv H(z)/H_0, \tag{A1}$$

and integral

$$I(z) \equiv \int_0^z \frac{dz'}{E(z')}. \tag{A2}$$

For the a power law model, using Eq. (31), we have

$$\begin{aligned} I_1(z) &= \frac{2}{(2-m)D_3^{\frac{1}{2}}}[(1+z)^{-\frac{m}{2}+1} \\ &\quad \times F_1(\alpha_1, \beta_1, \gamma_1, \delta_1(1+z)^{3-m}) \\ &\quad - F_1(\alpha_1, \beta_1, \gamma_1, \delta_1)], \end{aligned} \tag{A3}$$

where

$$\alpha_1 = \frac{2-m}{2(3-m)},\ \beta_1 = \frac{1}{2}, \tag{A4}$$

$$\gamma_1 = \frac{8-3m}{2(3-m)},\ \delta_1 = -\frac{C_3}{C_2}, \tag{A5}$$

and $F_1(\alpha,\beta,\gamma,x)$ represents the hypergeometric function.

For the H power law model, using Eq. (66), we obtain

$$\begin{aligned} I_2(z) &= H_0^{-1}(1+z)\frac{2}{(2-m)D_3^{\frac{1}{2}}}[(1+z)^{-\frac{m}{2}+1} \\ &\times F_1(\alpha_1,\beta_1,\gamma_1,\delta_1(1+z)^{3-m}) \\ &-F_1(\alpha_1,\beta_1,\gamma_1,\delta_1)]. \end{aligned} \tag{A6}$$

APPENDIX B: DATA ANALYSIS FOR THE NUMERICAL FITTING

We utilize several data sets to constrain the parameters of the two power law model. The free parameters in these two models are power law index m (or n), current value of fractional energy density of dark matter Ω_{m0}, and the current value of h ($h = H_0/100/km\cdot s^{-1}\cdot Mpc^{-1}$). However, since the current value of Hubble parameter h is always around 0.70 which is determined by current supernovae constraints so we marginalize it and plot the contour maps of power index m and n versus Ω_{m0}. Our data sets include 307 high quality "Union" SN Ia data, baryon acoustic oscillation measurement from the Sloan Digital Sky Survey, 9 observational $H(z)$ data and the shift parameter from WMAP three years results.

1. Selected high quality SN Ia data set

The first standard candle we use is the type Ia supernovae (SNe Ia), which is published by Supernova Cosmology Project (SCP) team recently [37]. This data set contains 307 selected SNe Ia that includes several current widely used SNe Ia data, such as Hubble Space Telescope (HST) [3, 38], SuperNova Legacy Survey (SNLS) [39, 40] and the Equation of State: SupErNovae trace Cosmic Expansion (ESSENCE) [41]. The likelihood function can be determined by χ^2 statistics, for the type Ia supernovae

$$\chi^2_{\rm SN} = \sum_{i=1}^{182}\frac{(\mu_{th}(\text{parameters};z_i)-\mu^{(i)}_{\rm exp})^2}{\sigma_i^{*2}}, \tag{B1}$$

where

$$\mu_{th}(\text{parameters};z) = 5\log d_L(z) + 25, \tag{B2}$$

where d_L is the luminosity distance which is determined by Eq. (A2)

$$d_L(z) = (1+z)\int_0^z \frac{dz'}{H(z')} = H_0^{-1}(1+z)I(z). \tag{B3}$$

2. Baryon Acoustic Oscillation measurement from SDSS

In the large-scale clustering of galaxies, the baryon acoustic oscillation signatures could be seen as a standard ruler providing the other important way to constrain the expansion history of the Universe. We use the measurement of the BAO peak from a spectroscopic sample of 46,748 luminous red galaxies (LRGs) observations of SDSS to test cosmology [42], which gives the value of $A = 0.469(n_s/0.98)^{-0.35} \pm 0.017$ at $z_{\rm BAO} = 0.35$ where $n_s = 0.95$ [43]. The expression of A can be written as

$$\begin{aligned} A &= \frac{\sqrt{\Omega_{m0}}}{(H(z_{\rm BAO})/H_0)^{\frac{1}{3}}}[\frac{1}{z_{\rm BAO}}\int_0^{z_{\rm BAO}}\frac{dz'}{H(z')/H_0}]^{\frac{2}{3}} \\ &= \frac{\sqrt{\Omega_{m0}}}{E(z_{\rm BAO})^{\frac{1}{3}}}[\frac{I_{\rm BAO}}{z_{\rm BAO}}]^{\frac{2}{3}} \end{aligned} \tag{B4}$$

and the χ^2_{BAO} is

$$\chi^2_{BAO} = \Big(\frac{A-0.469(n_s/0.98)^{-0.35}}{0.017}\Big)^2. \tag{B5}$$

3. Observational H(z) Data (OHD)

By using the differential ages of passively evolving galaxies determined from the Gemini Deep Deep Survey (GDDS) and archival data [44], Simon et al. determined H(z) in the range $0 < z < 1.8$ [45].The 9 observational $H(z)$ pieces of data could be obtained from [45, 46] and they have been have been used to constrain the dark energy potential and equation of state [46]. The χ^2 statistics for these $H(z)$ data is

$$\chi^2_{\rm OHD} = \sum_{i=1}^{9}\frac{(H(\text{parameters};z_i)-H_i)^2}{\sigma_i^{*2}}. \tag{B6}$$

4. CMB Data from WMAP three years results

The CMB shift parameter may provide an effective way to constrain the parameters of dark energy models since it has the very large redshift distribution and be able to constrain the evolution of dark energy very well. The shift parameter R which is derived from the CMB data takes the form as

$$\begin{aligned} R &= \sqrt{\Omega_{m0}}\int_0^{z_{\rm CMB}}\frac{dz'}{H(z')/H_0} \\ &= \sqrt{\Omega_{m0}}I(z_{\rm CMB}) \end{aligned} \tag{B7}$$

The WMAP3 data gives $R = 1.70 \pm 0.03$ [47], thus we have

$$\chi^2_{\rm CMB} = \Big(\frac{R-1.70}{0.03}\Big)^2. \tag{B8}$$

To break the degeneracy and explore the power and differences of the constraints for these data sets, we use them in several combinations to perform our fitting: SN + BAO, SN + BAO + OHD, and SN + BAO + BAO + CMB.

[1] A. G. Riess *et.al*, Astron. J. **116**, 1009 (1998) [astro-ph/9805201]; S. Perlmutter *et.al.*, Astrophys. J. **517,** 565 **(**1999**)**

[2] C. L. Bennett *et al.,* Astrophys. J. Suppl. **148**, 213 (2003) [astro-ph/0302225]; D.N. Spergel *et al.,* ApJS. **170**, 377 (2007) [astro-ph/0603449]

[3] A. G. Riess *et al.*, Astrophys. J. **607**, 665 (2004) [astro-ph/0402512]

[4] J. M. Overduin and F. I. Cooperstock, Phys. Rev. D **58,** 043506 (1998) [astro-ph/9805260]; V. Sahni and A. A. Starobinsky, Int. J. Mod. Phys. D **9**, 373 (2000) [astro-ph/9904398]; K. Freese, New Astron. Rev. **49**, 103 (2005) [astro-ph/0501675]

[5] A. Strominger, Nucl. Phys. B **319**, 722 (1989); S. B. Giddings and A. Strominger, Nucl. Phys. B **307**, 854 (1988); B **321**, 481 (1989); M. D. Maia and G. S. Silva, Phys. Rev. D **50**, 7233 (1994) [gr-qc/9401005]; L. R. W. Abramo, R. H. Brandenberger and V. F. Mukhanov, Phys. Rev. D **56**, 3248 (1997) [gr-qc/9704037]; A. M. Polyakov, Int. J. Mod. Phys. 16, 4511 (2001) [hep-th/0006132]; T. R. Taylor and G. Veneziano, Nucl. Phys. B **345**, 210 (1990); I. L. Shapiro, Phys. Lett. B **329**, 181 (1994) [hep-th/9402150]; N.C. Tsamis and R. P. Woodard, Nucl. Phys. B **474**, 235 (1996) [hep-ph/9602315]; Phys. Lett. B **301**, 351 (1993); A. Bonanno and M. Reuter, Phys. Rev. D **65**, 043508 (2002) [hep-th/0106133]; Phys. Lett. B **527**, 9 (2002); I. G. Dymnikova and M. Yu. Khlopov, Mod. Phys. Lett. A **15**, 2305 (2000) [astro-ph/0102094]; I. G. Dymnikova and M. Yu. Khlopov, Eur. Phys. J. C **20**, 139 (2001)

[6] M. Özer and M. O. Taha, Phys. Lett. B **171**, 363 (1986); Nucl. Phys. B **287,** 776 (1987)

[7] W. Chen and Y. S. Wu, Phys. Rev. D **41**, 695 (1990), Erratum-ibid. D **45**, 4728 (1992)

[8] K. Freese, F. C. Adams, J. A. Frieman and E. Mottola, Nucl. Phys. B **287,** 797 (1987)

[9] J. C. Carvalho, J. A. S. Lima and I. Waga, Phys. Rev. D **46**, 2404 (1992)

[10] J. A. S. Lima and J. M. F. Maia, Mod. Phys. Lett. A **8**, 591 (1993)

[11] J. A. S. Lima and J. C. Carvalho, Gen. Relativ. Gravit. **26**, 909 (1994)

[12] T. Padmanabhan, Physics Reports **380**, 235 (2003) [hep-th/0212290]

[13] L. Amendola, M. Quartin, S. Tsujikawa, I. Waga, Phys. Rev. D **74,** 023525 (2006) [astro-ph/0605488]; G. Olivares, F. A. Barandela, D. Pavon, 0706.3860 [astro-ph]

[14] P. J. E. Peebles and Ratra, Astrophys. J. Lett. 325, L17 (1988); B. Ratra and P. J. E. Peebles, Phys. Rev. D **37,** 3406(1988); R. R. Caldwell, R. Dave and P. J. Steinhardt, Phys. Rev. Lett. **80,** 1582 (1998) [astro-ph/9708069].

[15] R. R. Caldwell, Phys. Lett. B **545**, 23 (2002) [astro-ph/9908168]

[16] B. Feng, X. L. Wang and X. M. Zhang, Phys. Lett. B **607**, 35 (2005) [astro-ph/0404224]; M. Z. Li, B. Feng and X. M. Zhang, JCAP **0512**, 002 (2005) [hep-th/0503268]; Z. K. Guo, Y. S. Piao, X. M. Zhang and Y. Z. Zhang, Phys. Lett. B **608**, 177 (2005) [astro-ph/0410654]; X. F. Zhang, H Li, Y. S. Piao and X. M. Zhang, Mod. Phys. Lett A **21**, 231 (2006) [astro-ph/0501652]; B. Feng, M. Z. Li, Y. S. Piao and X. M. Zhang, Phys. Lett. B **634**, 101 (2006) [astro-ph/0407432]

[17] D. Huterer and M. S. Turner, Phys. Rev. D **60**, 081301(R) (1999) [astro-ph/9808133]

[18] S. Tsujikawa, Phys. Rev. D **72**, 083512 (2005) [astro-ph/0508542]

[19] Z. K. Guo, N. Ohta and Y. Z. Zhang, Phys. Rev. D **72**, 023504 (2005) [astro-ph/0505253]

[20] J. A. S. Lima, J. V. Cunha and J. S. Alcaniz, Phys. Rev. D **68**, 023510 (2003) [astro-ph/0303388]; T. Padmanabhan Phys. Rev. D **66**, 021301(R) (2002). [hep-th/0204150]; M. Sahlén, A. R. Liddle and D. Parkinson, Phys. Rev. D **75**, 023502 (2007) [astro-ph/0610812]; M. Sahlén, A. R. Liddle and D. Parkinson, Phys. Rev. D **72**, 083511 (2005) [astro-ph/0506696]

[21] S. Nojiri, S. D .Odintsov and H. Stefancic, Phys. Rev. D **74**, 086009 (2006) [hep-th/0608168]; G. Esposito-Farèse and D. Polarski, Phys. Rev. D **63**, 063504 (2001) [gr-qc/0009008]; B. Boisseau, G. Esposito-Farèse, D. Polarski, A. A. Starobinsky, Phys. Rev. Lett. **85**, 2236 (2000) [gr-qc/0001066]

[22] N. Dalal, K. Abazajian, E. Jenkins and A. V. Manohar, Phys. Rev. Lett. **87**, 141302 (2001) [astro-ph/0105317]; A. P. Billyard and A. A. Coley, Phys. Rev. D **61**, 083503 (2000) [astro-ph/9908224]; L. Amendola, *ibid.* **62**, 043511 (2000) [astro-ph/9908023]; W. Zimdahl and D. Pavon, Phys. Lett. B **521**, 133 (2001) [astro-ph/0105479]; D. Tocchini-Valentini and L. Amendola, Phys. Rev. D **65**, 063508 (2002) [astro-ph/0108143]; D. Comelli, M. Pietroni and A. Riotto, Phys. Lett. B **571**, 115 (2003) [hep-ph/0302080]; X. Zhang, Phys. Lett. B **611**, 1 (2005) [astro-ph/0503075]; X. Zhang Mod. Phys. Lett. A **20**, 2575 (2005) [astro-ph/0503072]

[23] J. M. F. Maia and J. A. S. Lima, Phys. Rev. D **65**, 083513 (2002) [astro-ph/0112091]

[24] L. P. Chimento, A. S. Jakubi, D. Pavón and W. Zimdahl, Phys. Rev. D **67**, 083513 (2003) [astro-ph/0303145]; A. P. Billyard and A. A. Coley, Phys. Rev. D **61**, 083503 (2000) [astro-ph/9908224]; L. Amendola, Phys. Rev. D **60**, 043501 (1999) [astro-ph/9904120]; L. Amendola and C. Quercellini, Phys. Rev. D **68**, 023514 (2003) [astro-ph/0303228]; W. Zimdahl and D. Pavón, Gen. Rel. Grav. **35**, 413 (2003) [astro-ph/0210484]; L. Amendola, C. Quercellini, D. T. Valentini and A. Pasqui, Astrophys. J. **583**, L53 (2003) [astro-ph/0205097]; W. Zimdahl, D. Pavón and L. P. Chimen, Phys. Lett. B **521**, 133 (2001) [astro-ph/0105479]

[25] V. Silveira and I. Waga, Phys. Rev. D **50**, 4890 (1994)

[26] A. Sen, Phys. Scr. T **117**, 70 (2005)

[27] V. Silveira and I. Waga, Phys. Rev. D **56**, 4625 (1997) [astro-ph/9703185]; J. A. S. Alcaniz and J. M. F. Maia, Phys. Rev. D **67**, 043502 (2003) [astro-ph/0212510]

[28] S. Nesseris and L. Perivolaropoulos, Phys. Rev. D **70**, 043531 (2004) [astro-ph/0401556]

[29] J. S. Alcaniz and J. A. S. Lima, Phys. Rev. D. **72**, 063516 (2005) [astro-ph/0507372]

[30] R. A. Daly *et.al*, ApJ **677** (2008) 1, 0710.5345 [astro-ph]

[31] A. Melchiorri, L Pagano and S. Pandolfi, Phys. Rev. D. **76** (2007) 041301(R), 0706.1314 [astro-ph]

[32] U. Alam, V. Sahni and A. A. Starobinsky, JCAP **0702** (2007) 011 [astro-ph/0612381]

[33] S. Nesseris and L. Perivolaropoulos, JCAP **01**, 018 (2007)

[astro-ph/0610092]
[34] V. Sahni, *et al.*, JETP Lett. **77**, 201 (2003); Pisma Zh. Eksp. Teor. Fiz. **77**, 249 (2003) [astro-ph/0201498]
[35] M. Li, Phys. Lett. B **603**, 1 (2004) [hep-th/0403127];X. Zhang, Phys. Lett. B **648**, 1 (2007) [astro-ph/0604484]; J. F. Zhang, X. Zhang and H. Y. Liu [astro-ph/0612642]; J. F. Zhang, X. Zhang, H. Y. Liu, Phys. Lett. B **651**, 84 (2007) [astro-ph/0706.1185]; X. Zhang, Phys. Rev. D **74**, 103505 (2006) [astro-ph/0609699]; Y. Z. Ma and X. Zhang, Phys. Lett. B **661**, 239 (2008), 0709.1517 [astro-ph]; Y. Z. Ma and Y. Gong and X. Chen, 0711.1641 [astro-ph].
[36] S.G. Djorgovski and V.G. Gurzadyan, Nucl. Phys. B **173** (2007) 6-10 [astro-ph/0610204]
[37] M. Kowalski et al., arXiv: 0804.4142 [astro-ph]
[38] A. G. Riess et al., Astrophys. J. **656**, (2007) [astro-ph/0611572]
[39] P. Astier et al., Astron. Astrophys. **447**, (2006) [astro-ph/0510447]
[40] S. Nesseris and L. Perivolaropoulos, JCAP. **0702**, 025 (2007) [astro-ph/0612653]
[41] W. M. Wood-Vasey et al., (2007) [astro-ph/0701041]
[42] D. J. Eisenstein et al., Astrophys. J. **633**, (2005) [astro-ph/0501171]
[43] D. N. Spergel et al., Astrophys. J. Suppl. Ser. **170**, 377 (2007) [astro-ph/0601133]
[44] R. G. Abraham et al. [GDDS Collaboration], Astron. J. **127**, 2455 (2004) [astro-ph/0402436].
[45] J. Simon, L. Verde and R. Jimenez, Phys. Rev. D **71**, 123001 (2005) [astro-ph/0412269]
[46] L. Samushia and B. Ratra, Astrophys. J. **650**, L5 (2006) [astro-ph/0607301]; H. Wei and S.N. Zhang, Phys. Lett. B **644**, 7 (2007) [astro-ph/0609597]
[47] Y. Wang and P. Mukherjee, 2007, astro-ph/0703780